Collisional formation and destruction of fast negative hydrogen ions in He, Ne, and Ar targets

D. P. Almeida,* N. V. de Castro Faria, F. L. Freire, Jr.,
E. C. Montenegro, and A. G. de Pinho
Departamento de Física, Universidade Católica do Rio de Janeiro, 22453, Rio de Janeiro, Brazil
(Received 19 December 1986)

Measurements are reported of the cross sections for collisional destruction (single- and double-electron loss) of H^- and for its formation through single- and double-electron capture by H and H^+, respectively. Three different targets were employed (He, Ne, and Ar) and the velocity (in a.u.) of the projectiles was $2.4 \leq v \leq 12.6$ for H^+ and $4 < v < 9$ for H and H^-. The charge states emerging from the target were simultaneously detected and the data were analyzed by the growth rate and attenuation methods from which individual cross sections could be deduced. Special attention was paid to the double-capture process in Ar where a very pronounced shell effect was firmly established on experimental grounds and was successfully described by theoretical estimates based on independent-electron probabilities of capture and simple scaling rules. Difficulties for obtaining an overall description of the cross sections for either destruction or formation of H^- based on simple models are discussed.

I. INTRODUCTION

The negative ion of hydrogen is a weakly bound system characterized by an electron affinity of 0.755 eV. This ion can be formed in collisions involving hydrogen species as projectiles either through single-electron capture (SEC) by neutral atoms or through double-electron capture (DEC) by protons. Its destruction results from two competitive processes: single- and double-electron loss (SEL and DEL, respectively). In the present work the charge-changing cross sections, $\sigma_{0\bar{1}}$ for SEC, $\sigma_{1\bar{1}}$ for DEC, $\sigma_{\bar{1}0}$ for SEL, and $\sigma_{\bar{1}1}$ for DEL, were measured with H^+, H, and H^- beams impinging upon gaseous targets of He, Ne, and Ar. The beams were obtained from the vertical-mounting 4-MV Van de Graaff accelerator at Pontificia Universidade Católica do Rio de Janeiro. The energy range that can be spanned goes, in principle, from 0.15 MeV/u (for D^+ projectiles) up to 4 MeV/u (for H^+ projectiles) but for technical reasons, to be explained below, this energy interval was not fully accessible for all the incident beams.

The fact that the ground state is the unique bound state of H^- simplifies the study of collisional formation of this ion: Once it is observed, its state is known unambiguously. When dealing with H^- as the initial or final state of a collision, it is interesting to investigate how far one can describe this negative ion by a single-parameter wave function which would make easy the use of an effective charge as a scaling factor in the description of cross sections. As will be shown later, this question makes sense regardless of the fact that the two electrons are strongly correlated[1] and the correlation cannot be explained even by two interacting s electrons.[2] Another important question is to what extent two-electron transfer processes can be treated as a two-step process[3,4] in the sense that the two-electron probability can be written as the product of two one-electron probabilities. This question can be examined in the double capture by a proton from a multielectron atom and in the double loss from H^-. Experimental evidence to answer these questions is relatively scarce. In addition, almost all the experimental studies on the formation or destruction of H^- were performed until now with low-velocity projectiles. Therefore, extensive measurements of one- and two-electron transfer cross sections with H^- as either the initial or the final state, over a broad range of velocities and with different targets, are warranted. A review of the experimental situation up to 1973 is presented by Tawara and Russek.[5]

The SEL cross section has been already measured by different authors[6–9] for He and Ar in the energy range covered by the present work but results for Ne are presented for the first time. For all targets the measured SEL cross sections are systematically smaller than those calculated by the free-collision model (FCM).[10] The FCM describes the electron-loss process as the scattering of the projectile electron by the target. The incident electron is assumed to be moving freely and with the same velocity as the projectile nucleus. Detachment occurs if the energy transfer, as measured in the rest frame of the projectile nucleus, exceeds the ionization energy. It is worth mentioning that this model correctly describes the electron loss of a neutral hydrogen projectile (the σ_{01} cross section) suggesting that probably there are deficiencies in the simplified treatment of the electron-electron correlation adopted by Dewangan and Walters[10] in their description of H^-. Our results for DEL at energies larger than 0.6 MeV are new for all targets; only a few data were previously reported[7] for He. The FCM was not yet extended to the DEL case.

Experimental results for SEC in the three targets and for DEC in Ne are presented for the first time. Additional data for DEC in He and Ar were also obtained in this work. For this last target a conspicuous shell effect was conclusively established with the present measurements of DEC cross sections for energies larger than 1 MeV. The

paucity of DEC data[11,12] comes from the fact that this process has a very small probability. At 1 MeV, for example, $\sigma_{1\bar{1}}$ for protons on He is 6 orders of magnitude smaller than the neutralization cross section σ_{10}. This ratio decreases rapidly with increasing energy.

The description of the electron-capture process is far from being a trivial problem even in the simplest case of reactions of the form $A^+ + B\ (n'l'm') \rightarrow A\ (n,l,m) + B^+$ where A^+ and B^+ are bare nuclei and A and B are hydrogenic systems. This three-body problem received its first quantal treatment in an oversimplified version of the first Born approximation known nowadays as the Oppenheimer-Brinkman-Kramers (OBK) approximation. This approximation was worked out by many authors and its more refined version is due to Nilolaev[13] who extended the approximation to deal with multielectron target atoms. Many interesting features experimentally observed in $H^+ + B \rightarrow H + B^+$ reactions with the contributions from the different shells of the target atom B considered altogether are qualitatively reproduced. A remarkable feature[11,13,14] is a shoulder around 500 keV in the σ_{10} cross section in Ar. However, it was clear since the beginning that the OBK approximation[15] was not adequate to deal with the two collisions associated with the Thomas double-scattering mechanism. In addition, in the MeV/u region results from Nikolaev[13] are systematically larger by a factor of about 3 than the experimental data. Moreover, it was demonstrated recently[16,17] that the OBK amplitude is not even a correct single-collision-capture amplitude. Besides involving unnecessary shortcomings, it does not take into account the correct asymptotic form of the scattering wave functions. It seems now that a correct first-order Born approximation[16,17] reproduces well the absolute values of K-K cross sections in the intermediate energy range, where the Thomas mechanism is not important and the forward scattering is dominant.

A second-order theory, the continuum–distorted-wave (CDW) approximation introduced by Cheshire,[18] was extended by Belkić *et al.*[19] for systems more complex than those including only hydrogen and helium species as both projectile and target, and an extensive comparison between theory and experiment was presented for total, partial, and differential capture cross sections. Good general agreement was achieved but the firmly established distinctive shoulder in the σ_{10} total cross section for Ar was not correctly reproduced.

Meanwhile, Macek and Alston[20,21] developed a new approximation for the calculation of the cross section for one-electron capture from a hydrogenlike ion of large nuclear charge by a bare ion, namely, the strong-potential Born approximation (SPB). In this approximation the capture process is described as a two-step reaction in which the electron is virtually ionized in the field of the target nucleus and then is attached to the projectile ion. It is essentially a second-order Born approximation and is called strong potential because the capture goes via intermediate states of the stronger target potential. Some of the earliest difficulties of the SPB calculations which were circumvented by the peaking approximation[20] are well understood presently.[22] As a matter of fact, the SPB-peaking approximation describes correctly the σ_{10} cross section for K-shell capture from C, Ne, and Ar by protons.[20,23].

Two-electron-capture cross-section calculations are still more complex and were restricted for a long time to collisions of H^+ or He^{2+} projectiles with H_2 or He targets. Lin[24] was the first to try the description of double-capture cross sections of neon K electrons by bare projectiles. To account for the two-step mechanism in which double capture proceeds through two single-electron transfers, he adopted a three-state two-center atomic expansion calculation. Order-of-magnitude agreement was obtained with the available experimental data. Gayet *et al.*[3] extended the CDW approximation to describe L-K double transfer from Ar to F^{9+} projectiles with good quantitative agreement at energies around 3 MeV/u. However, it must be stressed that there is no available calculation concerning the double transfer from multielectron atoms to H^+ projectiles. In this paper results for K-K single-electron capture by protons were used to calculate DEC cross sections for Ne and Ar taking advantage of OBK scaling rules and considering the incomplete shells in the same way as Nikolaev[13] did. The purpose was to check some simple ideas concerning the independent-electron treatment of the double transfer at intermediate energies (~ 1 MeV/u) and the use of only one effective charge in the description of the two electrons of H^-. A short and preliminary version of this work has been presented[25] elsewhere.

II. EXPERIMENTAL APPARATUS AND MEASUREMENT TECHNIQUES

The cross sections have been obtained by the growth rate method. In a three-component system, such as hydrogen, six charge-changing processes are possible, characterized by the cross sections σ_{ij} ($j \neq i$ with $i,j = -1,0,+1$). When $j = 0$, ground and excited states are considered altogether. Individual cross sections can be obtained if a beam consisting of only one charge state i is prepared and sent through a collision chamber. The new charge states j that appear in the emergent beam are then observed at the lowest possible pressures. Let Π represent the number of atoms of target gas per centimeter squared which the beam has traversed. This quantity is proportional to the pressure inside the collision chamber. If the pressure is so low that the probability that a beam particle undergoes more than one atomic collision during its traversal of the target is negligible, then the initial rate of growth of the fraction $F_j(\Pi)$ will be linear, with slope equal to σ_{ij} (in cm^2). Even when this single-collision condition is not strictly satisfied and two-collision processes are not so improbable, the cross sections can be deduced from the data. By neglecting higher-order collisions, it follows that

$$[F_j(\Pi) - F_j(0)]/\Pi = \sigma_{ij} + B\Pi \ , \tag{1}$$

where $F_j(0)$ is the fraction of the state of charge j measured in the absence of target gas. The parameter B describes the effect of double collisions. The left-hand side of Eq. (1) can be obtained experimentally. Plotting this quantity against Π and extrapolating to $\Pi = 0$ gives the charge-transfer cross section.

To indicate the quality of the rough data, Fig. 1 shows some typical growth curves obtained with rather different combinations of incident beam, impact energy, gas target, and detection system.

The preparation of pure and sufficiently intense incident beams is required. The H^+ beam was accelerated with the 4-MV electrostatic accelerator and magnetically analyzed in mass and energy. Capture cross section depends strongly on the energy; therefore, good energy resolution is mandatory. The energies of the analyzed incident beams were known with an accuracy better than 0.15% above 1 MeV. Below this energy the accuracy is increasingly poorer attaining 1% at 0.3 MeV. Beams in the range 0.15–0.30 MeV/u were obtained with deuterons and care was exercised to avoid trouble with the H_2^+ contamination.

The analyzed beam was collimated by two sets of staggered crossed pairs of micrometric sliding slits 100 cm apart. A typical value of the beam dimension after collimation was 0.5×0.5 mm^2. The beam entered a large chamber through an insulated $\phi_1=1.5$ mm diaphragm followed by a 2.5-mm antihalo aperture. The exit aperture of the chamber was 5 mm in diameter. The entrance and exit diaphragms also played the role of vacuum impedances to the line.

The chamber was a differentially pumped gas cell consisting of a high-pressure target chamber inside the larger chamber backed by a 170-liter/sec turbomolecular pump mounted directly underneath the gas cell. The target cell was 10 cm in length and the electrically insulated entrance and exit apertures had a diameter of $\phi_2=1$ mm. The target cell was coupled to a two-axis goniometer making its alignment easy. The ratio of the currents intercepted by the entrance and exit diaphragms to the emergent current was better than 1:1000. The target cell was provided for the gas inlet, the gas pressure gauge and a surface barrier detector for monitoring the scattered projectiles. Pressures in the gas cell were monitored with a thermocouple carefully calibrated for each gas against a liquid-nitrogen-trapped McLeod gauge whose mercury was cooled to about 0 °C in order to effectively eliminate the pumping action of mercury streaming to the cold trap.[5,26] The pressure in the target cell could be varied from 2 to 200 mTorr. Pumping speed coupled with the dimension of the apertures was such that a pressure differential of nearly 1000:1 was obtained across the apertures. The pressure in the rest of the system was maintained around 10^{-6} Torr. The total uncertainty in the gas target thickness—compounded of estimate uncertainties in the absolute calibration of the McLeod gauge, the effective length of the gas cell, and the fluctuations in the calibration—was approximately ±10%. This was the largest source of error in the absolute cross sections.

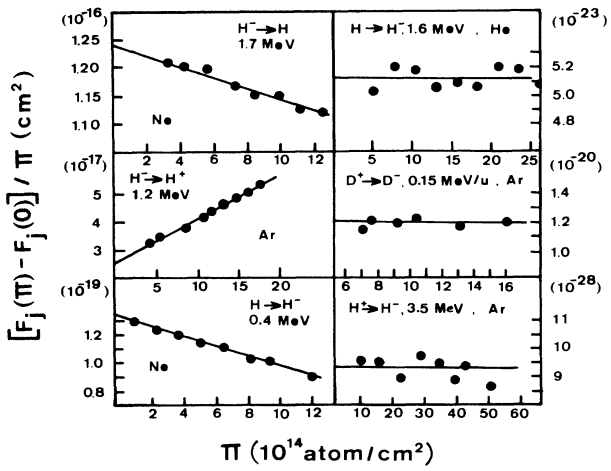

FIG. 1. Typical growth curves obtained for different combinations of projectile, target, and incident energy. The horizontal axis gives the target thickness in units of 10^{14} at/cm^2 and the vertical axis is $[F_j(\Pi)-F_j(0)]/\Pi$ in cm^2/atom.

The neutral beam was produced by the breakup of H_2^+ ions. Therefore, its energy is limited to 2 MeV. This procedure gives a much more intense beam than those produced by neutralization of proton beams. For this purpose a second differentially pumped gas cell was mounted right after the stabilizing slits. Air was introduced into this cell and the pressure was chosen to maximize the intensity of the neutral beam. Downstream of the dissociation cell, the charged fragments in the emerging beam were removed by the deflecting field of a permanent magnet. Some of the neutral atoms resulting from the H_2^+ breakup are not in the ground state. The distance from the dissociation cell to the target chamber was about 200 cm. Thus the flight time from one cell to the other was long compared to the radiative lifetime of all hydrogen atoms with $n\lesssim6$ except for those in the metastable $2s$ state. The fractions of highly excited neutral atoms that happen to reach the collision cell can be neglected since their population is roughly proportional to n^{-3}. On the other hand, when particles with velocity **v** traverse a magnetic field with field lines perpendicular to **v**, they experience a motional electric field. For a velocity corresponding to 1-MeV protons, the electric field associated with our permanent magnet amounted to about 1 kV/cm and it was fairly constant over a distance of 6 cm along the beam. This field can strongly quench H($2s$) atoms formed either directly or by cascading. Thus most of the H atoms arriving at the target cell are in the ground state.

To be sure of this assertion, we measured the electron-loss cross section σ_{01} as it is very different for atoms in the $2s$ and $1s$ states. Our results, which are in excellent agreement with previously reported ones[5] for H($1s$), are compared in Fig. 2 with the FCM predictions.[10]

The negative ion beam was produced by the breakup of H_3^+ and H_2^+ ions. Before being momentum analyzed by the 90° magnet, the molecular beams were sent into a third differentially pumped gas cell where they were destroyed. The relative large yield of H_3^+ ions from a dirty rf source and the enhanced probability of producing H^- ions from the breakup of H_3^+ lead to a copious production of negative fragments. With neutral and negative beams some apertures were modified, namely, $\phi_1=2.5$ mm and $\phi_2=3$ mm.

The target gases were claimed by the manufacturers to be 99.99% pure. For Ne and Ar this purity was high enough to ensure correct measurements of the cross sec-

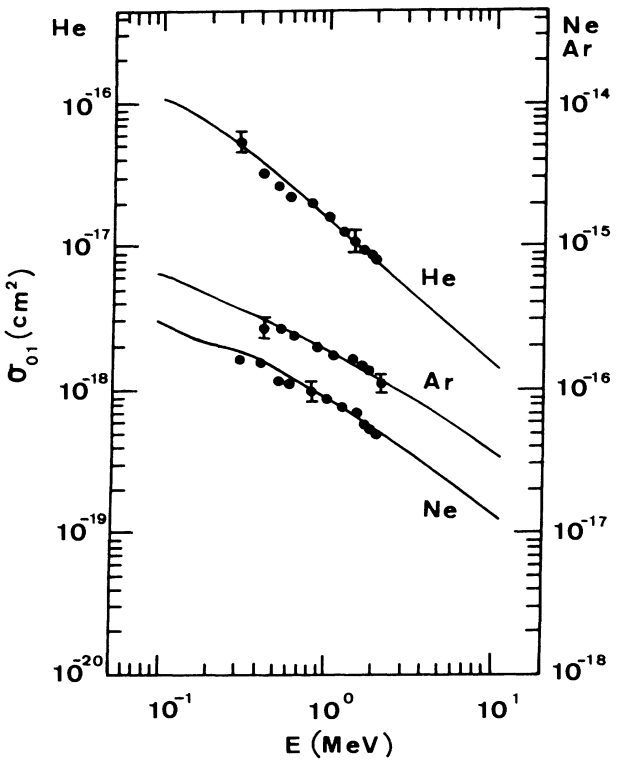

FIG. 2. One-electron-loss cross section σ_{01} measured in this work. The curves are FCM predictions (Ref. 10). Some typical error bars are shown.

tions. However, for He the small concentrations of impurities are significant because DEC cross sections of some of the contaminants are larger than that of He by a factor of about 100 at 1 MeV. Thus the $\sigma_{1\bar{1}}$ cross section for He was not measured above this energy.

The mixed beam emerging from the collision chamber was split into its charge-state components in the switching magnet and the latter were simultaneously collected at 0° and ±30°. The negative ions were detected by a 250-mm^2 surface barrier detector. The positive and neutral beams were measured either with Faraday cups or with surface barrier detectors depending on their intensities. Before entering the Faraday cup the neutral beam went through a grounded aluminium-coated Mylar foil and a negatively biased guard ring. The Faraday cups were 3.75 cm wide and 30 cm long and were located at the border of the switching magnet whose residual field was very efficient in preventing secondary electrons from leaving or entering the cups. The angular acceptance of the detectors was such that even for the highest pressures in the target cell and for the lowest velocities of the incident beam, the fraction of scattered particles not reaching the detectors was negligible. The distance from the target to the detection system was about 150 cm and the vacuum in the switching magnet was kept around 10^{-6} Torr.

With all the charge-state components fully and simultaneously collected, the determination of charge fractions and then of the cross sections is easily accomplished by a linear least-squares fitting of $[F_j(\mathrm{II})-F_j(0)]/\mathrm{II}$. Uncertainties in the absolute values of the cross sections come from target thickness measurement, current measurements, and/or counting statistics, energy determination (especially in the extreme low energy region), and the fitting procedure. An average uncertainty of ±15% must be assigned to the absolute values of the cross sections measured in this work.

To check the internal consistency of the data, an alternative analysis was performed. For an incident beam in a given charge state the emergent fraction in the same charge state exhibits an exponential attenuation long before the equilibrium fraction is reached. The slope of the linear transmission curve obtained in a semilog plot gives directly the sum of the cross sections associated with the destruction of the incident beam. For neutral beams one obtains $\sigma_{01}+\sigma_{0\bar{1}}$ which is essentially equal to σ_{01} in the energy range under investigation. For negatively charged incident beams one gets the total collisional detachment cross section $\sigma_D=\sigma_{\bar{1}0}+\sigma_{\bar{1}1}$. Of course, the pressure must be low enough to prevent the initial charge state from being rebuilt by a second collision. However, in the present work the maximum pressure employed for each gas target was not high enough to allow a very precise determination

TABLE I. One-electron-loss cross sections σ_{01} (in units of 10^{-17} cm^2) obtained by the growth rate method (G) and by the attenuation method (T).

	$\sigma_{01}(10^{-17}\mathrm{cm}^2)$					
	He		Ne		Ar	
Energy (MeV)	G	T	G	T	G	T
0.3	5.40	5.51	17.6	18.0		28.9
0.4	3.55	3.43	15.5	16.6	27.6	27.2
0.5	2.74	2.76	12.0	12.0	28.0	25.8
0.6	2.40	2.58	11.2	11.3	23.3	24.4
0.8	1.83	2.04	9.76	9.50	20.6	21.3
1.0	1.38	1.53	8.52	8.63	18.0	19.0
1.2	1.27	1.37	7.36	7.35	16.0	16.6
1.4	1.08	1.10	6.90	7.01	14.5	14.5
1.6	1.00	1.08	6.25	6.01	13.6	14.1
1.8	0.84		5.52	5.49	12.6	13.0
2.0	0.81		5.25	5.28	10.6	11.0

TABLE II. Total detachment cross section σ_D (in units of 10^{-17} cm^2) obtained by the growth rate method (G) and by the attenuation method (T).

	σ_D (10^{-17} cm^2)					
	He		Ne		Ar	
Energy (MeV)	G	T	G	T	G	T
0.6	5.16	4.93	25.7	26.0	50.5	55.5
0.8	4.49	4.49	21.6	22.1		
0.9					38.8	42.3
1.0	3.65	4.00	18.1	18.7		
1.2	3.33	3.59	17.5	15.3	35.6	37.7
1.4	3.02	3.36	16.1	14.6		
1.5					31.1	31.9
1.7	2.58	2.60	12.9	13.4		
1.8					28.8	30.0
2.0					26.1	28.6

of σ_{01} and σ_D and the values presented in Tables I and II in the columns labeled T (for transmission) are affected by essentially the same uncertainties as those in the columns labeled G (for growth).

III. RESULTS AND DISCUSSIONS

A. SEL and DEL

Our measured values of $\sigma_{\bar{1}0}$ are presented in Table III. For Ar they agree well with the values of Rose *et al.*;[6] for He there are in the literature three reported values[7] inside the energy interval we studied and the agreement is also very good; for Ne there are no published values above 0.2 MeV. The ratio of the one-electron-loss cross sections $\sigma_{\bar{1}0}/\sigma_{01}$ is fairly independent of the energy, from 0.4 to 2.0 MeV, for Ar and Ne, being equal to 2.13 ± 0.15. For He this ratio is energy dependent, increasing from 2.1 at 0.6 MeV to 2.7 at 1.4 MeV. Both cross sections have been calculated[10] in the framework of the FCM. As shown in Fig. 2, this model reproduces correctly the experimental values of σ_{01}. However, the measured values of $\sigma_{\bar{1}0}$ lie systematically 20 to 40% below the calculated curves for the three gases in the range of energy from 0.075 to 2 MeV (see Fig. 3). For the targets under consideration there are many other experimental results[6–9] in this energy interval besides those reported in Table III.

The discrepancy is probably related to the description of the H^- structure adopted by Dewangan and Walters[10] who calculated $\sigma_{\bar{1}0}$ in two extreme situations. First, they considered the projectile as if it consisted of two equivalent loosely bound electrons. Second, the structure of the projectile was interpreted as consisting of a strongly bound electron, comparable to the $1s$ electron in H, and a very weakly bound electron. The experimental results clearly rule out the first description since it gives calculated values that even exceed those obtained with the second

TABLE III. SEL cross sections $\sigma_{\bar{1}0}$ in cm^2. Numbers in square brackets are powers of ten.

	$\sigma_{\bar{1}0}$ (cm^2)		
Energy (MeV)	He	Ne	Ar
0.4			5.60[−16]
0.5		2.68[−16]	
0.6	4.99[−17]	2.43[−16]	4.62[−16]
0.8	4.36[−17]	2.04[−16]	
0.9			3.57[−16]
1.0	3.55[−17]	1.72[−16]	
1.2	3.26[−17]	1.68[−16]	3.30[−16]
1.4	2.94[−17]	1.55[−16]	
1.5			2.90[−16]
1.7	2.53[−17]	1.24[−16]	
1.8			2.71[−16]
2.0			2.40[−16]

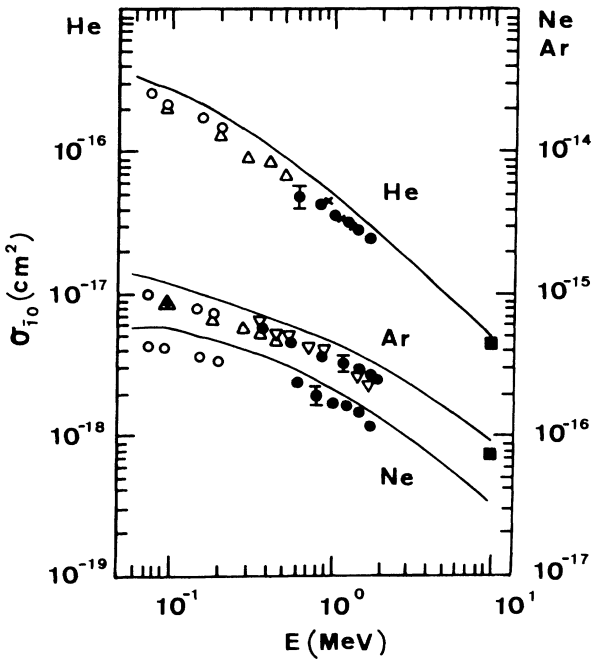

FIG. 3. Single-electron-loss cross section $\sigma_{\bar{1}0}$: ●, this work; ▽, Ref. 6; ×, Ref. 7; △, Ref. 8; ○ Ref. 9; ■, Ref. 28. The curves are FCM predictions (Ref. 10).

TABLE IV. DEL cross sections $\sigma_{\bar{1}1}$ in cm^2. Numbers in square brackets are powers of ten.

	$\sigma_{\bar{1}1}$ (cm^2)		
Energy (MeV)	He	Ne	Ar
0.4			5.81[−17]
0.5		1.89[−17]	
0.6	1.69[−18]	1.36[−17]	4.29[−17]
0.8	1.27[−18]	1.18[−17]	
0.9			3.13[−17]
1.0	9.63[−19]	9.30[−18]	
1.2	7.06[−19]	6.97[−18]	2.54[−17]
1.4	7.70[−19]	6.00[−18]	
1.5			2.08[−17]
1.7	4.70[−19]	5.30[−18]	
1.8			1.70[−17]
2.0			2.11[−17]

TABLE V. SEC cross sections $\sigma_{0\bar{1}}$ in cm^2. Numbers in square brackets are powers of ten.

	$\sigma_{0\bar{1}}$ (cm^2)		
Energy (MeV)	He	Ne	Ar
0.3	7.80[−20]		8.90[−20]
0.4	2.24[−20]	1.33[−19]	3.10[−20]
0.5	9.20[−21]	6.60[−20]	1.88[−20]
0.6	4.60[−21]	3.00[−20]	1.24[−20]
0.8	1.24[−21]	1.26[−20]	9.40[−21]
1.0	4.09[−22]	5.50[−21]	6.14[−21]
1.2	1.76[−22]	2.75[−21]	4.33[−21]
1.4	8.80[−23]	1.36[−21]	2.81[−21]
1.6	5.12[−23]	8.49[−22]	2.06[−21]
1.8	2.86[−23]	6.41[−22]	1.31[−21]
2.0	1.74[−23]	4.20[−22]	1.03[−21]

one. This lack of agreement is very disturbing since it persists at higher energies[27,28] where the FCM and the double-closure Born approximation of Gillespie[29,30] give the same results and there is no clear reason to expect the theory to fail. This result and the fact that $\sigma_{\bar{1}1}$ amounts to an important fraction of σ_D point to a very strong electron-electron correlation underlying the mechanism governing the electron loss from H^-.

The DEL cross section was not yet calculated in the FCM. Our experimental results are presented in Table IV. Except for three values given by Dimov and Dudnikov[7] for He around 1 MeV, there is no experimental result in the 0.6–2-MeV interval. In this interval the product $E\,\sigma_{\bar{1}1}$ is fairly constant for the three gases. Approximately the same value for this product is found[27,28] for Ar and He at energies 10 MeV showing that a v^{-2} dependence was already attained for energies greater than 0.6 MeV.

B. SEC and DEC

The SEC and DEC cross sections measured in the present work are given in Tables V and VI, respectively. Results for Ne in this energy interval are entirely new. In the limited range of energy examined, the SEC (0.4–2.0 MeV) and DEC (0.4–3.5 MeV) cross sections for Ne present a velocity dependence of v^{-7} and v^{-12}, respectively, which are about the same as those we have inferred for solid targets of carbon in this domain of velocities.[31] For

TABLE VI. DEC cross sections $\sigma_{1\bar{1}}$ in cm^2. Numbers in square brackets are powers of ten.

	$\sigma_{1\bar{1}}$ (cm^2)		
E (MeV)	He	Ne	Ar
0.15			(1.19±0.18)[−20]
0.20		(6.90±1.30)[−21]	(2.00±0.30)[−21]
0.25			(4.30±0.60)[−22]
0.30	(7.0±1.5)[−23]	(8.20±1.50)[−22]	(1.48±0.18)[−22]
0.40	(6.5±1.3)[−24]	(1.30±0.20)[−22]	
0.45		(6.40±0.90)[−23]	(3.82±0.50)[−23]
0.50	(8.6±1.5)[−25]		
0.60	(1.5±0.2)[−25]	(1.00±0.13)[−23]	(1.33±0.18)[−23]
0.70	(2.9±0.4)[−26]		
0.80	(1.5±0.2)[−26]	(1.55±0.20)[−24]	(4.53±0.55)[−24]
0.90			
1.00	(2.0±0.4)[−27]	(4.50±0.55)[−25]	(1.73±0.23)[−24]
1.20		(1.56±0.20)[−25]	(6.91±0.71)[−25]
1.30			(4.74±0.53)[−25]
1.40		(9.20±1.10)[−26]	(3.08±0.70)[−25]
1.60		(3.97±0.48)[−26]	(1.49±0.11)[−25]
1.80		(1.98±0.25)[−26]	(7.08±0.92)[−26]
2.00		(7.43±0.90)[−27]	(3.22±0.42)[−26]
2.50		(2.02±0.26)[−27]	(8.73±1.00)[−27]
3.00		(5.40±0.65)[−28]	(2.58±0.35)[−27]
3.50		(2.20±0.26)[−28]	(9.32±1.40)[−28]
4.00			(3.89±0.70)[−28]

He, the SEC results were extended up to 2 MeV and the DEC results confirm those of Schryber.[11]

The experimental data for Ar deserve some comments. It is well known that the single-electron-capture cross section from a given shell reaches a maximum when the velocity of the projectile is of the order of the average velocity of the electron to be captured. After reaching this maximum, the partial cross section falls off rapidly. As the projectile velocity increases, the next inner shell begins to contribute significantly. When the total capture cross section is measured as a function of the projectile velocity, structures are often observed around the value of v for which the contribution of a given shell begins to be dominated by that of the inner shell. This peculiar feature was observed[11,14] in the neutralization of protons traversing an Ar target. It is, in this case, associated with the transition from dominant M to dominant L regime.[13] The same effect is nicely observed for both SEC and DEC cross sections presented in this paper.

C. An approximate calculation of $\sigma_{1\bar{1}}$

An estimate of the total cross section for double charge transfer from a multielectron atom to a fast proton to form the negative ion H^- can be obtained assuming that the electrons are captured independently. An impact parameter description of the one-electron transfer probability is justified for dealing with total cross sections. The cross section for the formation of H^- (in its ground state represented by ξ) when a proton captures two electrons from the target atom A, one from the state α and other from the state β, can be written as

$$\sigma(A(\alpha,\beta),\xi)=2\pi\int_0^\infty bP_{A\alpha,\xi}(b)P_{A\beta,\xi}(b)db\ , \tag{2}$$

where $P_{A\alpha,\xi}$, and $P_{A\beta,\xi}$ are the velocity-dependent one-electron probabilities and α,β stands for the complete set of quantum numbers necessary to specify the state. The nuclear charges are $Z_1=1$ for the projectile and Z_2 for the target.

An evaluation of (2) starting from first principles is beyond the scope of this work and some simplifications will be introduced. The first ones concern the atomic wave functions. The ground state of H^- is often described[1] by a $(1s)^2$ wave function which has two different nuclear-charge parameters to simulate electron-electron correlations. Angular correlation, despite its importance,[2] will not be taken into account in our model. In the target atom the passive electrons are considered to form a frozen core during the capture of the active electron. The active electron will be described by a hydrogenic wave function which takes into account inner and outer screening due to the passive electrons. The inner screening is considered through a shell-dependent effective charge Z_α. Making explicit all relevant variables and parameters one may write $P_{A\alpha,\xi}=P(b,Z_1=1,Z_2,\alpha(Z_\alpha)\rightarrow\xi)$.

Collisions for which the first-order process is dominant correspond to impact parameters smaller than the average atomic radius of the active electron. The projectile acts as a probe of the higher momentum components of the wave function and a satisfactory estimate of $P_{A\alpha,\xi}(b)$ can be obtained with no more than a good knowledge of the wave functions in the inner region of the atom. This is also true for the emerging negative ion, a particularly extended system. This fact can be used to simplify to a greater degree the description of the H^- state ξ. If the electron density at the origin calculated with the Chandrasekhar wave function is equalized to that calculated with a $(1s)^2$ hydrogenic wave function, one can replace the two nuclear-charge parameters by a single one, viz., $Z_1^*=0.582$. The same argument can be invoked to justify that the effective target charge Z_α is that for which the corresponding hydrogenic wave function gives the same average value of $1/r$ as the relativistic Hartree-Fock calculations,[32] namely, $Z_\alpha=n_\alpha^2\langle 1/r\rangle_{\mathrm{RHF}}$. It is better to choose $\langle 1/r\rangle$ instead of $\langle r\rangle$ to give the adequate weight to the higher momentum components. Then a more compact notation can be used for the one-electron probability, that is,

$$P_{A\alpha,\xi}=P(b,Z_1^*,Z_\alpha,n_\alpha\rightarrow n_\xi=1)\ , \tag{3}$$

where it is implied that the incident particle is a proton and that the electron in the emergent particle has principal quantum number $n_\xi=1$ and is in the Coulomb field due to Z_1^*. On the other hand, the target active electron is in the quantum state α, with principal quantum number n_α in the field due to Z_α.

Despite its well-known limitations, the OBK approximation is very useful in suggesting scaling rules which are widely and successfully employed.[15,33] To render more transparent these scaling rules and the use that will be made of them, some results of the OBK are briefly recalled here. The total cross section *averaged* over all initial $(2n^2)$ and final (2) angular momentum states can be written as [the notation of Eq. (3) and atomic units will be used thereafter]

$$\bar{\sigma}_{\mathrm{OBK}}(Z_1^*,Z_\alpha,n_\alpha\rightarrow n_\xi=1)=2^7\pi(Z_1^*)^3(Z_\alpha/n_\alpha)^5/5v^2\gamma_\alpha^5\ , \tag{4}$$

where

$$\gamma_\alpha\simeq\frac{v^2}{4}\left[1+\frac{(Z_\alpha/n_\alpha)^2}{v^2}\right]^2 \tag{5}$$

because for protons on Ne or Ar the collision is very asymmetric.

Then it follows[15,33] that

$$\bar{\sigma}_{\mathrm{OBK}}(Z_1^*,Z_\alpha,n_\alpha\rightarrow 1)=\bar{\sigma}_{\mathrm{OBK}}(Z_1^*,Z_\alpha/n_\alpha,1\rightarrow 1)\ . \tag{6}$$

To proceed further it is assumed that this scaling rule holds also for the probabilities

$$P(b,Z_1^*,Z_\alpha,n_\alpha\rightarrow 1)=P(b,Z_1^*,Z_\alpha/n_\alpha,1\rightarrow 1)\ . \tag{7}$$

Considering that the $K\rightarrow K$ probability for capture by protons in the OBK approximation is given by[15]

$$P(b,Z_1^*,Z_K,1\rightarrow 1)=[2b^4(Z_1^*)^3Z_K^5/v^2\gamma_K^2]K_2^2(b\gamma_K^{1/2})\ , \tag{8}$$

the integral (2) can be evaluated by using Eqs. (4) to (8). To this end, two cases must be considered separately: (i) both electrons come from the same shell S, and (ii) the

electrons come from different shells S and S'.

In the first case, the two probabilities appearing in Eq. (2) are equal to each other. Making use of the scaling rule (7) and introducing (8) into Eq. (2), it follows that, for each pair of electrons, the double-capture cross section in this case is equal to

$$\bar{\sigma}_{SS}=(5^2\lambda/2^{11}\pi)\gamma_S\bar{\sigma}_S^2 , \tag{9}$$

where the factor $\lambda=5.44$ results from the numerical integration. Following Nikolaev,[13] γ_S must be redefined as γ_S^* by substituting the hydrogenic energy $(Z_S/n_S)^2$ by the experimental[34] binding energy ε_S. In this way, the outer screening is partially taken into account. In addition, if there are N_S electrons in the shell all the different possibilities must be counted. Let σ_s be the *total* cross section for the single-electron capture by a *proton* from shell S. The total double-capture cross section for two electrons from S will be given by

$$\sigma_{SS}=[(N_S-1)/N_S](5^2\lambda/2^{13}\pi)(Z_1^*)^6\gamma_S^*\sigma_S^2 . \tag{10}$$

If the active electrons belong to different shells, another approximation can be made by noting that for values of b for which the probability associated to the inner shell S begins to fall off to negligible values, the probability associated with the outer shell S' remains still almost constant. Then $P_{S'}(b)$ can be replaced by the value of Eq. (8) calculated at the limit $b\to 0$ after performing the convenient scaling. Upon inserting this result into Eq. (3) and using (4) it is found that

$$\bar{\sigma}_{SS'}=\left[\frac{5}{16\pi}\right]\gamma_{S'}\bar{\sigma}_{S'}\bar{\sigma}_S . \tag{11}$$

With the same definitions as before and taking into account the number of electrons available in S and S', one has

$$\sigma_{SS'}=\left[\frac{5}{32\pi}\right](Z_1^*)^6\gamma_{S'}^*\sigma_{S'}\sigma_S . \tag{12}$$

Scaling rules and other results from OBK were used to obtain Eqs. (10) and 12). However, an important point to be emphasized is that we assume that (i) once σ_S and $\sigma_{S'}$ are known from *any* theory, Eqs. (10) and (12) connect single- to double-electron transfer cross sections, and (ii) if, at least, σ_K is known from any theory or even by fitting curves to experimental data, obtained for many different targets, the scaling rule (6) can be used to generate other single-capture cross sections.

As the K-electron capture from Ne and Ar are well described by the SPB peaking approximation and the theoretical cross section is given in a closed form,[20] this approach was adopted to estimate the double-capture cross sections. Thus the single-electron-capture cross section from the shell S by a proton will be written as

$$\sigma_S=N_S\sigma_{\mathrm{SPB}}(Z_1=1,Z_S/n_S,\varepsilon_S,K\to K) , \tag{13}$$

where σ_{SPB} is the cross section per electron.

These expressions must be used with care. The OBK scaling rule is valid for a cross section averaged over the initial states. If the shell is incomplete the scaling is no longer valid. This is the case for the Ar M-shell where the $3d$ subshell is empty. Nikolaev[13] has given relations between incomplete- and complete-shell cross sections within his modified OBK approximation (to be designated as OBKN). In particular one can obtain the ratio

$$\frac{\sigma_{\mathrm{OBKN}}(Z_1,Z_M,\varepsilon_M,3s+3p\to K)}{\sigma_{\mathrm{OBKN}}(Z_1,Z_M,\varepsilon_M,n=3\to K)}=F_M . \tag{14}$$

A crucial test for the scaling rules is to obtain σ_{10} for Ne and Ar starting from $\sigma_{\mathrm{SPB}}(K\to K)$. Figure 4 compares

$$\sigma_{10}(\mathrm{Ne})=2\sigma_{\mathrm{SPB}}(1,Z_K,\varepsilon_K,K\to K)+8\sigma_{\mathrm{SPB}}(1,Z_L/2,\varepsilon_L,K\to K)$$

with experimental data (open symbols). Our data for σ_{10}(Ne) are given in Table VII. Figure 5 does the same thing for

$$\sigma_{10}(\mathrm{Ar})=8\sigma_{\mathrm{SPB}}(1,Z_L/2,\varepsilon_L,K\to K)+8F_M\sigma_{\mathrm{SPB}}(1,Z_M/3,\varepsilon_M,K\to K) .$$

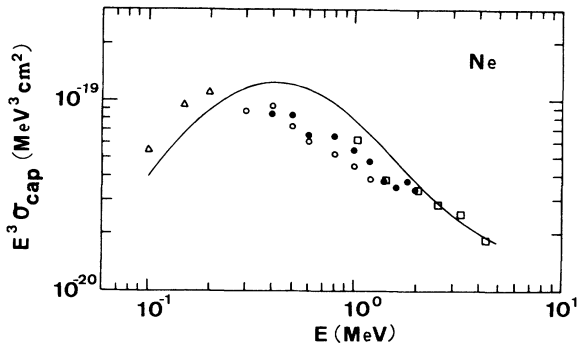

FIG. 4. One-electron-capture cross sections in Ne. Open symbols refer to σ_{10}: □, Ref. 11; △, Ref. 35; ○, this work. Solid symbols refer to $2\sigma_{0\bar{1}}/(Z_1^*)^3$: ●, this work. The curve is explained in the text.

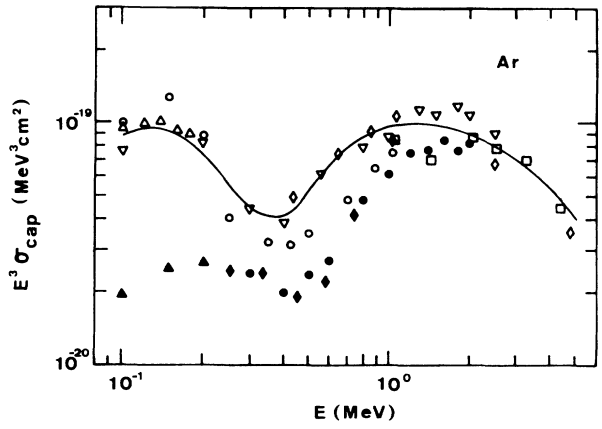

FIG. 5. The same as in Fig. 4 for Ar. σ_{10}: □, Ref. 11; ○, Ref. 35; ▽, Ref. 14; △, Ref. 36; ◇, Ref. 37. $2\sigma_{0\bar{1}}/(Z_1^*)^3$: ●, this work; ▲, Ref. 9; ◆, Ref. 11.

TABLE VII. One-electron-capture cross section σ_{10} (in units of 10^{-20} cm^2) for Ne.

E (MeV)	0.3	0.4	0.5	0.6	0.8	1.0	1.2
σ_{10} (10^{-20} cm^2)	324	144	58.0	28.0	10.2	4.42	2.22

In both figures the calculated and experimental cross sections were multiplied by E^3 in order to eliminate partially the strong velocity dependence of the capture cross sections. Excellent agreement is reached, especially for Ar for which a remarkable structure is predicted. It is worth mentioning that from 0.1 to 5 MeV the σ_{01} cross section spans 6 orders of magnitude and all experimental points appearing in Fig. 5 are concentrated into a single decade, showing that the agreement between experimental and calculated results is quite significant. The same figures show also the experimental results (solid symbols) for $\sigma_{0\bar{1}}$. In this case, in order to compare $\sigma_{0\bar{1}}$ with σ_{10}, the experimental results were multiplied by two to take into account the fact that only one final state is available and divided by $(Z_1^*)^3$ to correct for the charge acting upon each electron in the final state. The data for Ne are not very conclusive and one can say that an overall reasonable agreement was reached. However, for Ar the impossibility of describing the experimental results from 0.1 to 2.0 MeV with a single energy-independent scaling factor is obvious. The effective charge scales well the data for which $E \gtrsim 0.4$ MeV but it fails to describe the low-energy region.

The DEC cross sections are presented in Figs. 6 and 7. Now, all the cross sections were multiplied by E^6. The structure in the cross section observed experimentally around 0.5 MeV for Ar is very well reproduced by these simple calculations. Again it must be stressed that the experimental values of $\sigma_{1\bar{1}}$ condensed in Fig. 7 cover 8 orders of magnitude.

IV. CONCLUSIONS

In this work a systematic study of the collisional formation and destruction of the negative hydrogen ion was performed. The targets were noble gases (He, Ne, and Ar) and the velocities (in a.u.) of the projectiles were in the interval from 2.4 to 12.6. A great amount of new experimental information is presented and the following conclusions can be drawn: (i) the single-electron-loss (SEL) cross section is systematically lower by a factor of about 1.3 than the predictions of the free-collision model; however, except for this scaling factor they are as well described by the model as the σ_{01} cross section; (ii) the double-electron-loss (DEL) cross section exhibits a v^{-2} dependence for velocities from 5 up to ~ 20 a.u. and becomes increasingly smaller than the SEL cross sections as the velocity of the projectile increases; (iii) it is not possible to relate the single-electron-capture (SEC) cross sections $\sigma_{0\bar{1}}$, and σ_{10} by a single velocity-independent scaling factor playing the role of effective charge specially in the low-velocity regime; (iv) double-electron-capture (DEC) seems to proceed through two independent single-electron transfers; (v) SEC and DEC processes in Ar exhibit around $v = 5$ the same shell effect already observed in σ_{10}, which is related to the transition from a regime of dominant M-electron capture to one of dominant L-electron capture; (vi) the σ_{10} and $\sigma_{1\bar{1}}$, cross sections for Ar are remarkably well reproduced with a simple model which incorporates the idea of two-step transfer and scaling rules from the Nikolaev OBK formulation and uses as input K-K cross sections obtained from the strong-potential Born peaking approximation; and (vii) the behavior of $\sigma_{0\bar{1}}$ and $\sigma_{1\bar{1}}$ cross sections for He in the limited energy range

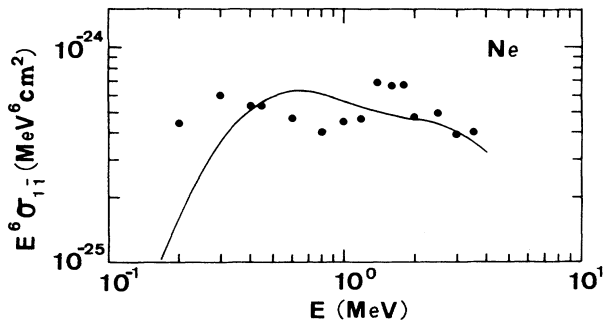

FIG. 6. Two-electron-capture cross section in Ne. ●, this work. The curve is explained in the text.

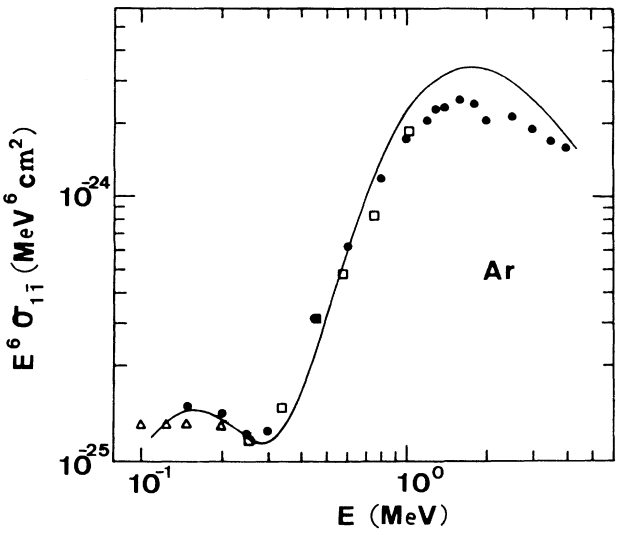

FIG. 7. The same as in Fig. 6 for Ar. ●, this work; □, Ref. 11; △, Ref. 12.

explored in this work is different from that observed with multielectron targets. A more rigorous treatment of these few-body problems is a much better approach than the description of the electronic states through one-parameter hydrogenic wave functions and the SPB approximation.

ACKNOWLEDGMENTS

This work was supported in part by Financiadora de Estudos e Projetos and Conselho Nacional de Desenvolvimento Científico e Tecnológico, Brazilian governmental agencies.

---

*Permanent address: Instituto de Física, Universidade Federal do Rio de Janeiro, Brazil.

[1]S. Chandrasekhar, Astrophys. J. **100**, 176 (1944).

[2]F. Borondo, A. Macias, and A. Riera, Chem. Phys. **81**, 303 (1983).

[3]R. Gayet, R. D. Rivarola, and A. Salin, J Phys. B **14**, 2421 (1981).

[4]V. A. Sidorovich, V. S. Nikolaev, and J. H. McGuire, Phys. Rev. A **31**, 2193 (1985).

[5]H. Tawara and A. Russek, Rev. Mod. Phys. **45**, 178 (1973), and references therein.

[6]P. H. Rose, R. J. Conner, and R. P. Bastide, Bull. Am. Phys. Soc. II **3**, 40 (1958).

[7]D. I. Dimov, and V. G. Dudnikov, Zh. Tekh. Fiz. **36**, 1239 (1966) [Sov. Phys.—Tech. Phys. **11**, 919 (1967)].

[8]J. Heinemeir, P. Hvelplund, and. F. R. Simpson, J. Phys. B **9**, 2669 (1976).

[9]C. J. Andersen, R. J. Girnis, A. M. Howald, and L. W. Anderson, Phys. Rev. A **22**, 822 (1980), and references therein.

[10]D. P. Dewangan and H. R. J. Walters, J. Phys. B **11**, 3983 (1978).

[11]V. Schryber, Helv. Phys. Acta. **40**, 1023 (1967).

[12]L. H. Toburen and M. Y. Nakai, Phys. Rev. **177**, 191 (1969).

[13]V. S. Nikolaev, Zh. Eksp. Teor. Fiz. **51**, 1263 (1966); [Sov. Phys.—JETP **24**, 847 (1967)].

[14]L. H. Toburen, M. Y. Nakai, and R. A. Langley, Phys. Rev. **171**, 114 (1968), and references therein.

[15]M. R. C. McDowell and J. P. Coleman, *Introduction to the Theory of Ion-Atom Collisions* (North-Holland, Amsterdam, 1970), Chap. 8.

[16]D. P. Dewangan and J. Eichler, J. Phys. B **19**, 2939 (1986).

[17]Dz. Belkić, R. Gayet, J. Hanssen, and A. Salin, J. Phys. B **19**, 2945 (1986).

[18]I. M. Cheshire, Proc. Phys. Soc. London **84**, 89 (1964).

[19]Dz. Belkić, R. Gayet, and A. Salin, Phys. Rep. **56**, 279 (1979).

[20]J. Macek and S. Alston, Phys. Rev. A **26**, 250 (1982).

[21]S. Alston, Phys. Rev. A **27**, 2342 (1983).

[22]D. P. Dewangan and J. Eichler, J. Phys. B **18**, L65 (1985).

[23]E Horsdal-Pedersen, C. L. Cocke, J. L. Rasmussen, S. L. Varghese, and W. Waggoner, J. Phys. B **16**, 1799 (1983).

[24]C. D. Lin, Phys. Rev. A **19**, 1510 (1979).

[25]D. P. Almeida, N. V. de Castro Faria, F. L. Freire, Jr., E. C. Montenegro, and A. G. de Pinho, Bull. Am. Phys. Soc. **31**, 1302 (1986); Nucl. Instrum. Meth. B (to be published).

[26]H. Ishii and K. Nakayama, in *Transactions of the Eighth National Vacuum Symposium* (Pergamon, New York, 1961), p. 519.

[27]R. Symthe and J. W. Toevs, Phys. Rev. **139**, A15 (1965).

[28]K. H. Berkner, S. Kaplan, and R. N. Pyle, Phys. Rev. **134**, A1461 (1964).

[29]G. H. Gillespie, Phys. Rev. A **15**, 563 (1977).

[30]G. H. Gillespie, Phys. Rev. A **16**, 943 (1977).

[31]N. V. de Castro Faria, F. L. Freire, Jr., J.M.F. Jeronymo, E. C. Montenegro, A. G. de Pinho, and D. P. Almeida, Nucl. Instrum. Meth. B **17**, 321 (1986).

[32]C. C. Lu, T. A. Carlson, F. B. Malik, T. C. Tucker, and C. W. Nestor, Jr., At. Data 3, 1 (1971).

[33]W. E. Meyerhof, R. Anholt, J. Eichler, H. Gould, Ch. Munger, J. Alonso, P. Thieberger, and H. E. Wegner, Phys. Rev. A **32**, 3291 (1985).

[34]*Table of Isotopes,* 7th ed., edited by C. M. Lederer and V. S. Shirley (Wiley, New York, 1978).

[35]C. F. Barnett and K. H. Reynolds, Phys. Rev. **109**, 355 (1958).

[36]P. M. Stier and C. F Barnett, Phys. Rev. **103**, 896 (1956).

[37]L. M. Welsh, K. H. Berkner, S. N. Kaplan, and R. V. Pyle, Phys. Rev. **158**, 85 (1967).